Electronic Supplementary Material (ESI) for ChemComm.

Supplementary Information to:

Reversible and irreversible emergence of chiroptical signals in J-aggregates of achiral 4-sulfonatophenyl substituted porphyrins: Intrinsic chirality vs. chiral ordering in the solution

Oriol Arteaga,* Zoubir El-Hachemi, Adolf Canillas, Joaquim Crusats, Meritxell Rovira and
Josep M. Ribó*

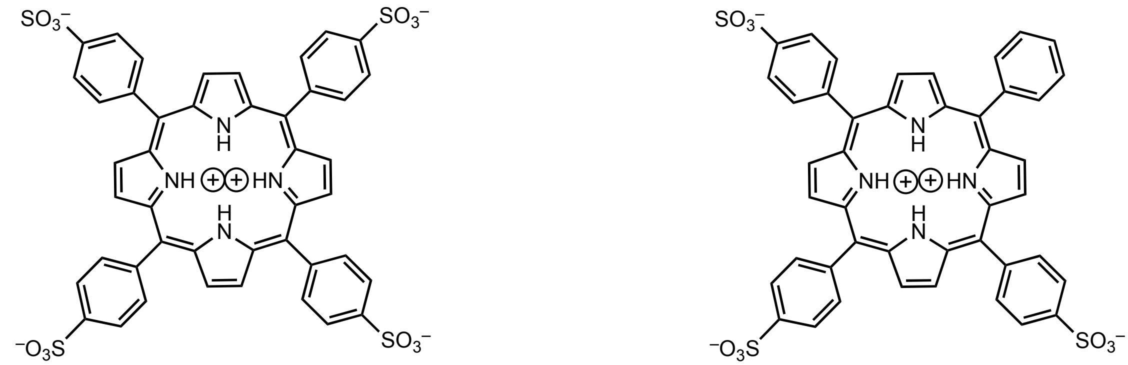

$H_2TPPS_4^{2-}$

$H_2TPPS_3^{-}$

Formula Scheme

Experimental details

Tetrasodium salts of $H_4TPPS_4^{2-}$ and $H_4TPPS_3^{-}$ were prepared as previously described in ref.[S1]. Zwitterionic $H_4TPPS_4^{2-}$ (absence of any metallic counter anion thant hydrated proptons and no anionic counter anions that those of the prophyrin sulfonato groups) was prepared as previously described in ref.[S2].

Solutions of $H_4TPPS_4^{2-}$ and $H_4TPPS_3^{-}$ J-aggregates (≈ 5 μM) composed by particles not showing linear polarizations were prepared by adding a mother porphyrin solution (≈ 1 mM) of the tetrasodium salt to a 0.2 M NaCl 0.1 M H_2SO_4 water solution: for examples on the CD signals obtained in different experimental conditions see below. The solutions of $H_4TPPS_4^{2-}$ J-aggregate nanotubes to study by Muellr matrix ellipsometry their behaviour in stirred solutions were prepared from zwitterionic $H_4TPPS_4^{2-}$ by capillary injection of the porphyrin mother solution in 0.01 M HCl solution as recently reported.[S3] In the case of the experiments with the trisodium salts of $H_4TPPS_3^{-}$ to yield samples composed by small rounded disks and plattes a drop of the mother solution was added to surface of a 0.2 M NaCl 0.1 M H_2SO_4 water solution. This in two type of conditions: stagnant solutions or magnetically stirrd solutions. Differences of the CD chiral sign of bisignate signals between this tow type of conditions are discussed in the principal text and show in Figs. S1. Experiments on $H_4TPPS_4^{-}$ solutions for the effects on the electronic spectra under magnetic stirring in clockwise (CW) or anticlockwise (CCW) stirring directions were performed in UV/Vis 1 cm square cuvette with a 4 mm x 0.7 mm magnetic bar.

UV/Vis spectra were recorded on a Cary-Varian 5E instrument. Circular dichroism (CD) measurements for samples showing the absence of linear polarization properties, as determined by Mueller matrix ellipsometry, were recorded on a Jasco J-815 CD spectropolarimeter. Mueller matrix polarimetry and Mueller matrix microscopy are decribed below.

Experimental conditions and details on the stirring experiments for the reversible stirring effect as observed by Mueller matirx polarimetry were as described in refs.[2f,h,k].

Sonication pulse experiments were performed using a Bradson Digital Sonifier (Danbury, CT, USA) Model 250. Pulse sequences either of 0.5 s or 3 s each minute were used. Sample obsration were perforemd about each 8 hours during one day. Figs. below show examples of the influence of this under and in the absence of stirring. Experiments for the effect of sonication under magnetic stirring in clockwise (CW) or anticlockwise (CCW) stirring directions on H4TPPS$_3^{-}$ solutions (see Figs. below) were performed in 49 ml solution in a 50 ml pyrex cylindrical flask (4 cm inner diameter: 30 mm x 7 mm magnetic bar).

The morphology of the J-aggregate particles was observed by atomic force microscopy (AFM) and peak force microscopy (PFM). See ref.[4] for instrumental and experimental details.

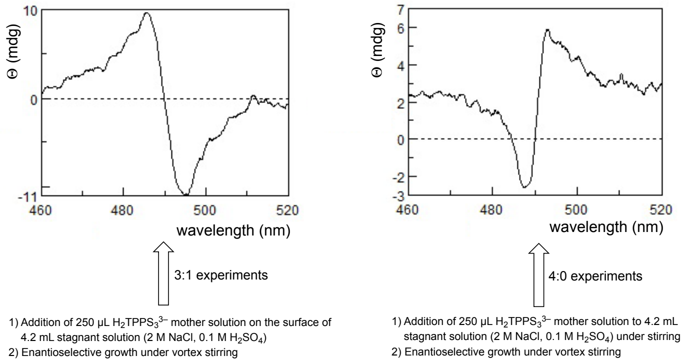

1) Addition of 250 μL $H_2TPPS_3^{3-}$ mother solution on the surface of 4.2 mL stagnant solution (2 M NaCl, 0.1 M H_2SO_4)
2) Enantioselective growth under vortex stirring

1) Addition of 250 μL $H_2TPPS_3^{3-}$ mother solution to 4.2 mL stagnant solution (2 M NaCl, 0.1 M H_2SO_4) under stirring
2) Enantioselective growth under vortex stirring

Fig. S1. The small change on the preparation method of adding the free base porphyrin mother solution to the acidic solution with stirring (right) or without sitirring (left) shows how the easier contact in the first aggregation stages with the water bulk determines the kinetic controlled effect of the chiral contaminant. The bisigante signal of the right is the common CD signal appearing in hundred of experiments, being attributed to a chiral contaminant present in purifired water, see ref.[9]

Mueller matrix polarimetry instruments

Spectroscopic

The spectroscopic Mueller matrix polarimeter[6a] that we have used has four photoelastic modulators (PEMs) that modulate the polarization state of light both before and after the sample. Fourier analysis of the time varying signal delivers simultaneously all sixteen elements of the Mueller matrix with very high precision. Fig. S2 shows a scheme of the instrument. Chiroptical measurements are made in the strait-through configuration.

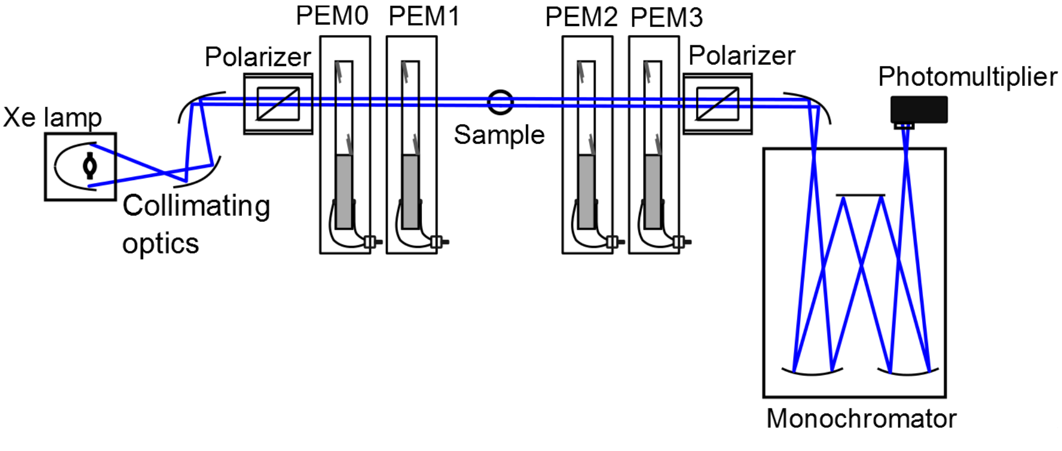

Fig. S2. Schematic of Mueller polarimetry device setup.

Space resolved/microscopy

The Mueller matrix (MM) microscope[6e] produces 16 images of a sample in around one minute. Each one of these images corresponds to a different element of the 4x4 Mueller matrix, providing the complete quantitative analysis of the modification of the polarization as the light beam is transmitted or reflected in the sample. False color is used to denote different magnitudes and signs in the MM elements. The MM microscope is able to measure the magnitude and orientation of linear dichroism and linear birefringence, the circular birefringence, the circular dichroism and the depolarization.

Our Mueller matrix microscope is based in the frequency analysis at the pixel level of the images continuously captured by a CMOS camera while two rotating compensators modulate the polarization of light. As the intensity detected by every individual pixel of the camera is frequency analyzed by digital demodulation, the determination of the optical properties keeps the same high lateral resolution of standard microscopy measurements.

Analysis of MMP data

In a *homogeneous* and non-depolarizing medium, the normalized Mueller matrix has at most six parameters. A non-depolarizing Mueller matrix is called a Mueller-Jones matrix and can be represented as follows:

$$M = \exp L = \begin{bmatrix} 0 & -LD & -LD' & CD \\ -LD & 0 & CB & LB' \\ -LD' & -CB & 0 & -LB \\ CD & -LB' & LB & 0 \end{bmatrix} \qquad \text{Eq. 1}$$

where, **L** is the differential Mueller matrix. The elements of **L** have a direct physical interpretation as the fundamental optical properties for light-matter interaction: LD - horizontal linear dichroism, LB - horizontal linear birefringence, LD´- 45º linear dichroism, LB´- 45º linear birefringence, CD - circular dichroism, and CB - circular birefringence.

This physical interpretation that we have provided for the elements of **L** corresponds to a medium that is homogenous in the direction of light propagation. In the case of *inhomogeneous* system, for example, a succession of misoriented thin layers, the representation given by equation (1) can be still valid but, in such conditions, the optical effects in **L** do not correspond to intrinsic fundamental properties of each layer. In this case the optical effects in **L** arise from the compounded effect of the different strata that compose the inhomogenous system. The stirred cuvette cannot be considered a homogeneous system because vortex flows clearly modify the alignment of the fibers as a function of the position they reach in the cuvette.

The stratified ordination of aggregates in the cuvette was simulated using a serial superposition of layers, each one of them represented by a different Mueller matrix. As it is described in the main manuscript, the cumulative result is given by:

$$\mathbf{M} = \mathbf{M}_{W-exit} \prod_{i}^{N} \mathbf{M}_{\mathrm{i,int}} \mathbf{M}_{W-input}$$

where N is the number of intermediate layers considered in the system. $\mathbf{M}_{\mathbf{W\text{-}input}}$ and $\mathbf{M}_{\mathbf{W\text{-}exit}}$ are, respectively, the Mueller matrices of the nanotubes at the input wall and exit wall of the cuvette. Their optical properties are discussed in the next section

MMP results of the wall deposits

Chiroptical signals

After prolonged stirring of the cuvette (> 12 hours) aligned nanoparticle aggregates are deposited on the cuvette walls. We verified (Fig S3) that empty cuvettes with wall deposits have remarkable chiroptical signals that vanish when one of the walls (input or exit) that interact with the light beam is cleaned. Thus, it is clear that such chiroptical signal arises due to the combined effect of the misoriented agglomerates and bundles of the straight J-aggregate nanotubes of $H_4TPPS_4^{2-}$ deposited at two successive cuvette walls. In this aspect, square cuvettes and cylindrical flask behave qualitatively equal.

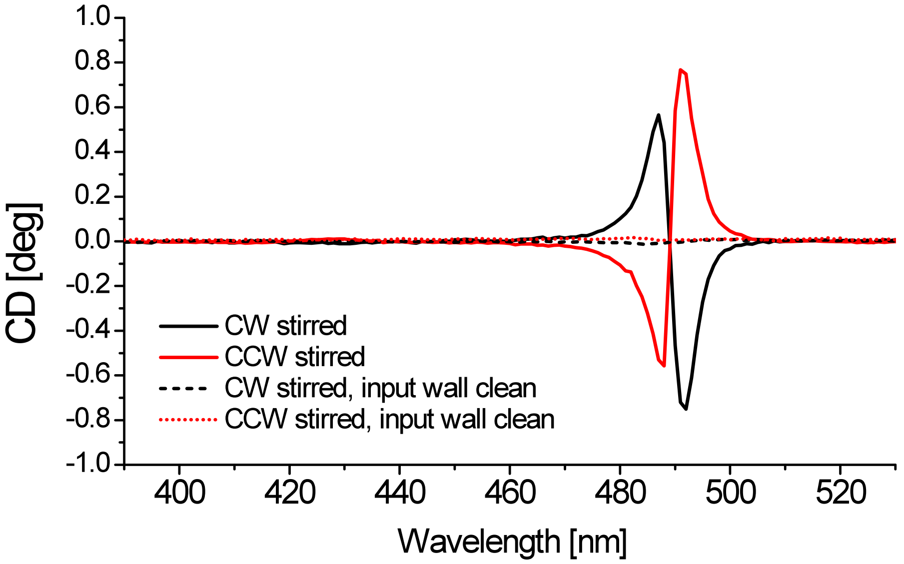

Figure S3. Chiroptical spectra of the wall deposited aggregates during stirring before and after cleaning one of the input walls.

Nanoparticle alignment

Fig. S4 a) shows the LD and LD' spectra for the deposit of the exit wall of a CW stirred cuvette. From these spectra the orientation of the linear dichroism can be easily calculated [angle = 0.5 x atan(LD'/LD)] and it is presented in figure b). Clearly the orientation of the 490nm J-band is close to -20º, while the H-band (at around 420 nm) is orthogonal to this band. For the input wall of the cuvette we obtained analog results (not shown in this Supplementary Information) but in that case the absorption of the J-band is oriented at around 20º.

The sample analyzed in Fig. S4 was measured again with the Mueller matrix microscope in order to take advantage of its high spatial resolution to distinguish the orientation of the fiber bundles. This measurement is shown in Fig. S5. Clearly it is possible to distinguish a main orientation of the bundles (marked with a red arrow in the unpolarized intensity image) that coincides with determined angle of orientation of the linear dichroism. Obviously, although the stirring mechanism is efficient orienting the fiber bundles deposited at the cuvette walls, some fibers are misoriented with respect to the main orientation. This causes some heterogeneity in the angular distribution of linear dichroism (last image of Fig. S5) but, on average, these results confirm our spectroscopic observations.

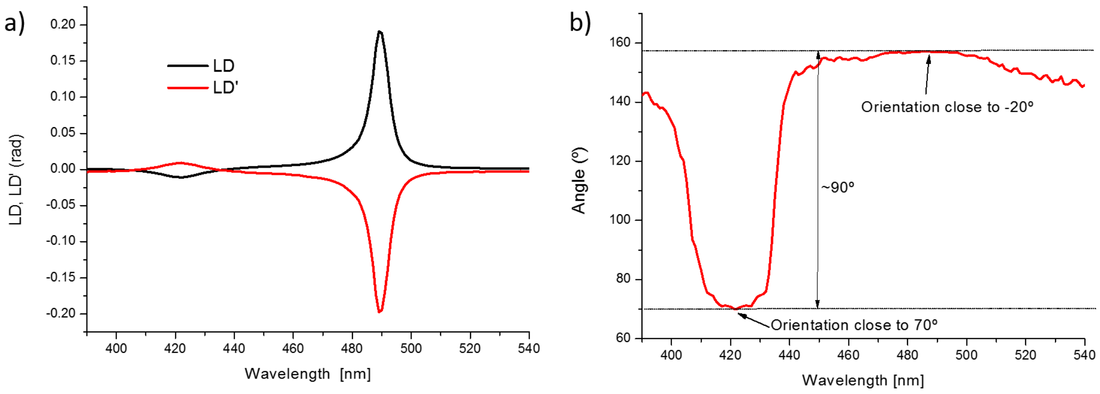

Fig. S4. LD and LD' (a) and calculated angle (b) for the deposit at the exit wall of a CW stirred cuvette.

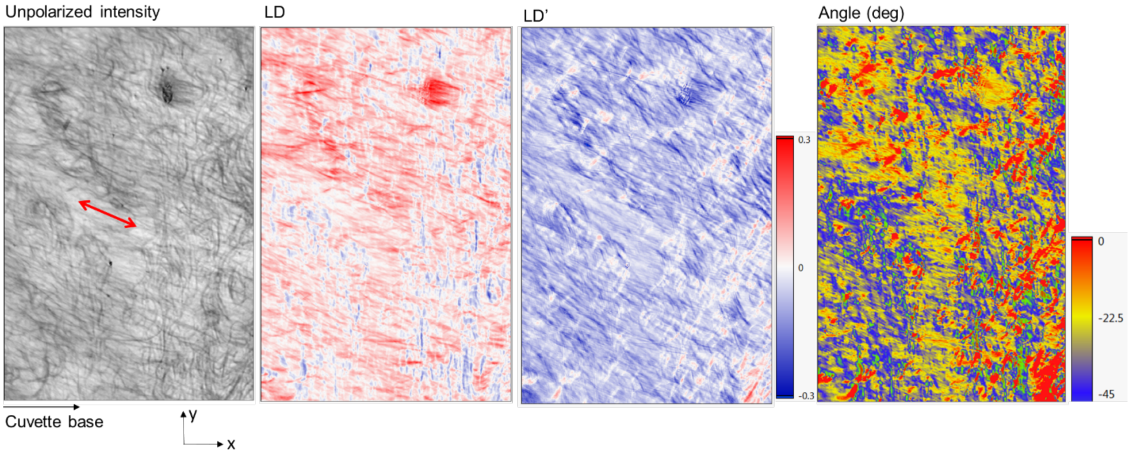

Fig S5. Alignment of the aggregate fiber bundles as seen with the Mueller matrix microscope using monochromatic light of 500 nm. The red arrow in the unpolarized intensity image indicates the main orientation of the fibers.

References Supplementary Information

S1 R. Rubires, J. Crusats, Z. El-Hachemi, T. Jaramillo, M. López, E. Valls, J.-A. Farrera and J. M. Ribo, *New J. Chem.* 1999, **23**, 189.

S2 C. Escudero, Z. El-Hachemi, J. Crusats and J. M. Ribo, *J. Porphyrins Phthalocyanines* 2005, **9**, 852.